A new model for rock blasting damage in tension through two-scale framework analysis

O. Keita[a,b], B. François[a] and C. Dascalu[c]

[a] *Building architecture and Town planning Departement (BATir) Universite Libre de Buxelles(ULB), Bruxelles, Belgique*
[b] *Laboratoire CRISMAT, UMR 6508, Université de Caen Basse-Normandie, Caen, France*
[c] *UPMC Université Paris, CNRS, Institut Jean Le Rond D'Alembert, Paris,France*
okeita@ ulb.ac.be.ac

Abstract

This paper proposes a new continuum damage model accounting for inertial effects (Keita et al 2014) to analyze the fracture behavior of rock in tension due to blasting. The two-scale damage model is fully deduced from small-scale descriptions of dynamic micro-cracks propagation under tensile loading (mode I). An appropriate micro-mechanical energy analysis is combined with homogenization based on asymptotic developments in order to obtain the macroscopic evolution law for damage (Dascalu et al 2008).

The global macroscopic response predicted by the model is obtained by implementation of the dynamic damage law in a transient finite elements code. The damage pattern around the blasthole was simulated. Numerical simulations were able to illustrate the ability of the model to reproduce the radial cracks zone due to rock blasting. The influences of microstructural size and of micro-cracks orientation on damage distribution around the blasthole have been determined.

Keywords: Micro-cracks, dynamic propagation, homogenization, dynamic damage, rock blasting.

1. Introduction

Rock fragmentation under blasting loads is a topic of great current interest and importance. It is a common practice in mining, quarries and construction industries. It also represents an index that is used to stimate the effect of bench blasting in the mining industry (Cho and Kaneko 2004). The blast induced-damage in the surrounding rock is a complex response and has to be well understood so that to better model the rock behavior under such a dynamic loading. The speed and high stress level of the loading are factors which complicate the establishment of appropriate damage law. In consequence, several intensive research activities have been carried out in the field of blast damage (Langefors and Kihlstrom 1978; Li et al. 2009). One of the ways to address this issue is the analysis of micro-structural damage process. The macroscopic damage evolution is due to micro-crack propagation that takes place at micro-scale. At that scale, the damage mechanism occurs in mode I (tension), even if the macroscopic loading is in compression (Brace and Bombalakis, 1963).

In the present paper, we propose a new approach for blasting damage of rocks. Considering the micro-crack dynamic propagation, the dynamic model of damage is deduced through the mathematical homogenization method based on asymptotic developments and locally periodic distribution of micro-cracks (Bensoussan et al., 1978; Sanchez-Palencia, 1980).

2. Two-scale problem

In this paper, we consider the dynamic evolution of the elastic solid containing a large number of micro-cracks. We suppose that the micro-crack distribution is locally periodic (see Fig. 1a). We denote by ε the size of a periodicity cell or, equivalently, the distance between the centers of neighbour micro-cracks and by l the micro-crack length. The length l is assumed to have small spatial variations

such that, locally, the distribution of micro-cracks may be considered as periodic. Each crack is assumed to be horizontal (parallel to the x_1-axis) and straight. We define the damage variable as the ratio between the micro-crack length l and the period size ε:

$$d = \frac{l}{\varepsilon} \tag{1}$$

The damage variable is necessarily included between 0 (for undamaged material) and 1 (for complete damaged material).

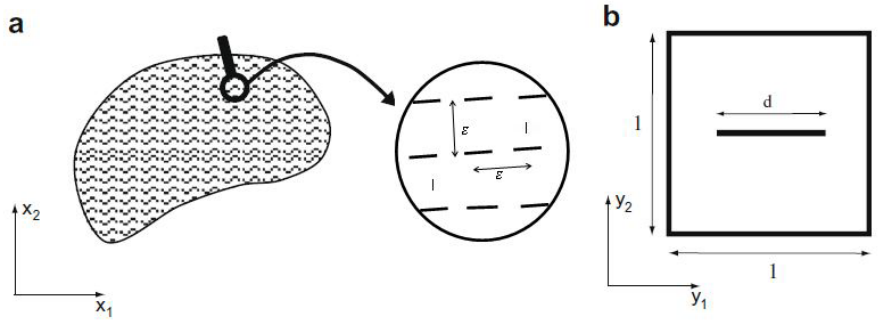

Fig.1. (a) Micro-fissured medium with locally periodic microstructure, ε is the size of a period and l is the local micro-crack length. (b) Unit cell with rescaled crack of length d.

3. Elastodynamics equations

We consider the elastodynamics equations for the initial heterogeneous medium that we assume to be a two-dimensional isotropic elastic medium containing a locally periodic array of micro-cracks. Let $\boldsymbol{B}_S = \boldsymbol{B}/\boldsymbol{C}$ be the solid part of $\boldsymbol{B}$, with $\boldsymbol{C}$ the union of all micro-cracks inside $\boldsymbol{B}$. The momentum balance equation is:

$$\frac{\partial \sigma_{ij}^{\varepsilon}}{\partial x_j} = \rho \frac{\partial^2 u_i^{\varepsilon}}{\partial t^2} \qquad \text{in} \qquad \boldsymbol{B}_s \tag{2}$$

including the linear elasticity constitutive relation:

$$\sigma_{ij}^{\varepsilon} = a_{ijkl}\, e_{xkl}(u^{\varepsilon}) \tag{3}$$

where a_{ijkl} is the elasticity tensor, $\sigma_{ij}^{\varepsilon}$ is the stress field and u^{ε} the displacement field from which the strain tensor is calculated in the small deformations hypothesis :

$$e_{xij}(\mathbf{u}^{\varepsilon}) = \frac{1}{2}\left(\frac{\partial u_i^{\varepsilon}}{x_j} + \frac{\partial u_j^{\varepsilon}}{x_i}\right) \tag{4}$$

On the lips of cracks, free opening contact under tension or friction conditions are assumed. These two alternatives are expressed respectively by the two sets of conditions.

$$\sigma^{\varepsilon}\mathbf{N} = 0 \quad \left[\mathbf{u}^{\varepsilon}.\mathbf{N}\right] > 0 \tag{5}$$

$$\left[\boldsymbol{\sigma}^{\varepsilon}\mathbf{N}\right] = 0 \quad \mathbf{N}.\sigma^{\varepsilon}\mathbf{N} < 0 \; \mathbf{T}.\sigma^{\varepsilon}\mathbf{N} = 0 \left[\mathbf{u}^{\varepsilon}.\mathbf{N}\right] = 0 \tag{6}$$

where $\mathbf{N}$ is a unit normal vector on the crack faces, $\mathbf{T}$ is the unit vector which is tangent to the crack

3.1 Asymptotic developments

The locally periodic microstructure is constructed from a reference unit cell Y (Fig.1b) referred to microscopic coordinates (y_1, y_2). Rescaled with the small parameter ε, the unit cell becomes the physical period of the material εY as in Fig. 2. We assume the microstructural period ε to be small enough with respect to the characteristic dimensions of the whole body and the wavelength of the elasto-dynamic field. In this case, we can distinguish between the microscopic and the macroscopic variations of the mechanical field. We consider distinct variables at different scales: the macroscopic variable x and the microscopic variable $y=x/\varepsilon$. For a variable depending on both x and y the total spatial derivative takes the form

$$\frac{d}{dx_i} = \frac{\partial}{\partial x_i} + \frac{1}{\varepsilon}\frac{\partial}{\partial y_i} \tag{7}$$

The unit cell Y contains the scaled crack CY and $Y_S = Y/CY$ its solid part. Following the method of asymptotic homogenization (e.g. Bensoussan et al. (1978); Sanchez-Palencia (1980)), we look for two-scale expansions of u^ε and σ^ε in the form:

$$u^\varepsilon(x,t) = u^{(0)}(x,y,t) + \varepsilon u^{(1)}(x,y,t) + \varepsilon^2 u^{(2)}(x,y,t) + \cdots \tag{8}$$

$$\sigma^\varepsilon(x,t) = \frac{1}{\varepsilon}\sigma^{(-1)}(x,y,t) + \sigma^{(0)}(x,y,t) + \varepsilon\sigma^{(1)}(x,y,t) + \cdots \tag{9}$$

where $= u^{(i)}(\mathbf{x},y,t)$ and $\boldsymbol{\sigma}^{(i)}(\mathbf{x},\mathbf{y},t)$), $\mathbf{x} \in$ B, $\mathbf{y} \in$ Y are smooth functions an Y - periodic in y.

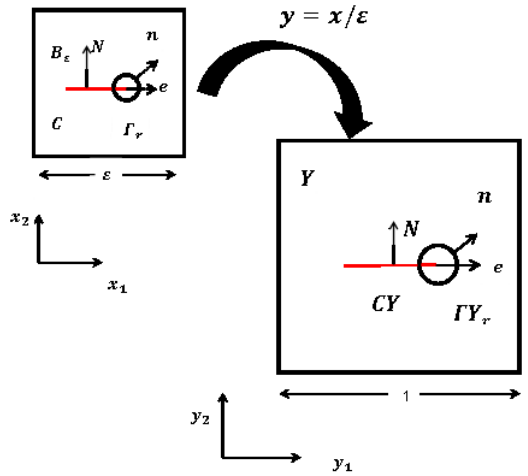

Fig.2. Rescaling of the unit cell to the microstructural period of the material.

3.2 Homogenization analysis

Substituting the asymptotic development of $\mathbf{u}^\varepsilon$ and $\boldsymbol{\sigma}^\varepsilon$ (Eq.7 and 8) in the elasto-dynamic Eq. (2, 3, 4) and taking into account the relation (6), one can obtain the followings expressions

$$\frac{\partial}{\partial x_j}\sigma_{ij}^{(I)} + \frac{\partial}{\partial y_j}\sigma_{ij}^{(I+1)} = \rho\frac{\partial^2 u_i^{(I)}}{\partial t^2} \tag{10}$$

$$\sigma_{ij}^{(I)} = a_{ijkl}\left(e_{xkl}\left(u^{(I)}\right) + e_{ykl}\left(u^{(I+1)}\right)\right) \tag{11}$$

that have to be solved for each I .

(i) Eq. (9) for I = -1 and Eq. (10) for I = 0 give:

$$\frac{\partial}{\partial x_j}\sigma_{ij}^{(0)} = 0 \tag{12}$$

$$\sigma_{ij}^{(0)} = a_{ijkl}\left(e_{xkl}\left(u^{(0)}\right) + e_{ykl}\left(u^{(1)}\right)\right) \tag{13}$$

For given $\mathbf{u}^{(0)}$, taking into account Eqs. (11-12) one obtains the boundary value problem for the corrector $\mathbf{u}^{(1)}$:

$$\frac{\partial}{\partial y_j}\left(a_{ijkl}e_{ykl}\left(u^{(1)}\right)\right) = 0, \qquad \text{in} \quad Y_s \tag{14}$$

$$\left(a_{ijkl}e_{ykl}\left(u^{(1)}\right)\right)N_j = -\left(a_{ijkl}e_{xkl}\left(u^{(0)}\right)\right)N_j, \quad \text{on } CY \tag{15}$$

with periodicity conditions on the external boundary of the cell. The microscopic corrector $\mathbf{u}^{(1)}$ depends linearly on the macroscopic deformations

$$u^{(1)}(x,y,t) = \xi^{pq}(y)e_{xpq}\left(u^{(0)}\right)(x,t) \tag{16}$$

Here the characteristic functions $\xi^{pq}(y)$ are elementary solutions of Eqs. (13-14) for the particular macroscopic deformations $e_{xkl}\left(\mathbf{u}^{(0)}\right)$. The equilibrium Eq. (11) shows that inertial effects are not directly present at the microscopic level.

(ii) Eq. (9) for I = 0 and Eq. (10) for I = 1 give

$$\frac{\partial}{\partial x_j}\sigma_{ij}^{(0)} + \frac{\partial}{\partial y_j}\sigma_{ij}^{(1)} = \rho\frac{\partial^2 u_i^{(0)}}{\partial t^2} \tag{17}$$

$$\sigma_{ij}^{(1)} = a_{ijkl}\left(e_{xkl}\left(u^{(1)}\right) + e_{ykl}\left(u^{(2)}\right)\right) \tag{18}$$

By applying the mean value operator $\langle . \rangle = \frac{1}{|Y|}\int_{Ys} .dy$ (here $|Y|$ is the area of Y) to Eq. (16) and remembering that $\mathbf{u}^{(0)}$ is y-independent, one can obtain:

$$\frac{\partial}{\partial x_j}\langle\sigma_{ij}^{(0)}\rangle = \langle\rho\rangle\frac{\partial^2 u_i^{(0)}}{\partial t^2} \tag{19}$$

We define the macroscopic stress

$$\langle\sigma_{ij}^{(0)}\rangle = \sum_{ij}^{(0)} \tag{20}$$

that can be expressed as

$$\sum_{ij}^{(0)} = C_{ijkl}e_{xkl}(\mathbf{u}^{(0)}) \tag{21}$$

where

$$C_{ijkl}^{\pm}(d) = \frac{1}{|Y|}\int_{Ys}\left(a_{ijkl} + a_{ijmn}e_{ymn}\left(\xi^{kl}\right)\right)dy \tag{22}$$

are the homogenized coefficients. We deduce the dynamic macroscopic behavior:

$$\frac{\partial}{x_j}\sum_{ij}^{(0)} = \langle\rho\rangle\frac{\partial^2 u_i^{(0)}}{\partial t^2} \tag{23}$$

as describing the overall dynamic behavior of an elastic body with a given distribution of (non-evolving) micro-cracks. These coefficients C_{ijkl} can be computed by solving the unit cell problems (13) and (14) for several d and interpolating between the obtained values. Those unit cell problems have been computed by the FEAP finite element code.

4. Energy release rate and dynamic damage evolution

We consider in this section the problem of evolving micro-cracks and we extend our homogenization method in order to obtain a macroscopic evolution law for damage.

4.1 Dynamic energy release rate

The dynamic energy release rate can be expressed at the tip of a micro-crack as follows

$$G^{d\varepsilon} = \lim_{r=0}\int_{\Gamma Yr}\left((U+T)n_1 - \sigma_{ij}^{\varepsilon}\frac{\partial u_i^{\varepsilon}}{\partial x_1}\right)ds \tag{24}$$

where

$$U = \frac{1}{2}a_{mnkl}\,e_{xkl}(u^{\varepsilon})\,a_{mnkl}\,e_{xmn}(u^{\varepsilon}) \tag{25}$$

$$T = \frac{1}{2}\rho\frac{\partial u^{\varepsilon}}{\partial t}\frac{\partial u^{\varepsilon}}{\partial t} \tag{26}$$

are respectively the energy of deformation and the density of kinetic energy (Freund, 1998). Here Γ_r is a circle of an infinitesimal radius r surrounding the crack tip and n is the unit normal vector on Γ_r (see Fig. 2).

The physical energy release rate in dynamics is expressed as function of the stress intensity factors as follows (Freund, 1998):

$$G^{d\varepsilon} = \frac{1-\nu^2}{E}A(\dot{l})k(\dot{l})^2(K_I^{\varepsilon})^2 \tag{27}$$

For crack propagation in mode I, Freund (1998) established the relation

$$A(\dot{l})k(\dot{l})^2 \approx \left(1-\frac{\dot{l}}{C_R}\right) \tag{28}$$

where c_R is Rayleigh wave speed and can be expressed by

$$c_R = \frac{0.862+1.14\nu}{1+\nu}\sqrt{\frac{E}{2(1+\nu)\rho}} \tag{29}$$

4.2 Dynamic damage evolution

Including the asymptotic development (7, 8) into relation (24), and comparing the obtained results with the physical energy release rate in dynamics (27), we establish the following equation

$$\frac{dd}{dt} = \frac{2C_R}{\varepsilon}\left(\frac{G^c}{\varepsilon*\frac{dC_{ijkl}}{dd}e_{xkl}(u^{(0)})e_{xij}(u^{(0)})} + \frac{1}{2}\right) \tag{30}$$

as the dynamic damage evolution law (see Keita et al. (2014) for more details).

5. Numerical implementation

Numerical implementation is done in a transient finite elements code with the combination of the following equations previously determined:

1. The dynamic macroscopic behavior

$$\frac{\partial}{x_j}\sum_{ij}^{(0)} = \langle\rho\rangle\frac{\partial^2 u_i^{(0)}}{\partial t^2} \tag{31}$$

with

$$\sum_{ij}^{(0)} = C_{ijkl}e_{xkl}(\mathbf{u}^{(0)}) \tag{32}$$

2. The dynamic damage evolution law

$$\frac{dd}{dt} = \frac{2C_R}{\varepsilon}\left(\frac{G^c}{\varepsilon * \frac{dC_{ijkl}}{dd}e_{xkl}(u^{(0)})e_{xij}(u^{(0)})} + \frac{1}{2}\right) \tag{33}$$

3. The irreversibility condition

$$\frac{dd}{dt} \geq 0 \tag{34}$$

The last condition expresses the fact that the micro-cracks can only increase in length during the deformation of the material.

The implicit management integration scheme is run by the numerical algorithm of the finite element code LAGAMINE. Here will just explain the implementation procedure which are 7 steps :

1. Application of the given load that generates the macroscopic deformation
2. The homogenized coefficients are calculated according to the crack is opening or closing under the load applied at point 1.
3. A new damage value is calculated from solving the dynamic damage equation (Eq. 33). If dd<0, dd=0 is imposed.
4. The homogenized coefficients are updated according to the new value of damage calculated in point 3.
5. The macroscopic stresses are calculated according to Eq. (32).
6. The tangent matrix is obtained via the variation of the homogenized coefficients

6. Blasting damage simulation

6.1 Blast load

The following explosion pressure time history has been considered:

$$P = P_d\left(\frac{d_c}{d_h}\right)^3 \frac{t}{t_r}e^{\left(1-\frac{t}{t_r}\right)} \tag{35}$$

where, d_c and d_h are the diameters of the explosive and blasthole (mm), respectively. P_d is the detonation pressure (Pa) which is the pressure exerted by the expansion of gases from the explosion. It can be calculated from the following equation, as suggested by the National Highway Institute (Konya and Walter 1991):

$$P_d = \frac{449.93 \times SGe \times VOD^2}{1+0.08SGe} \tag{36}$$

where, SGe is the density of the explosive (g/cm3), VOD is the detonation velocity of the explosive (m/s), t is the elapsed time, and t_r (= 0.0003361 s) is the time to reach peak pressure. The value of P_d, d_c and d_h are determined according to the type of explosive. In this study we consider the explosive Emulstar 3000 UG (see tab.1). Fig.3 shows the pressure time history corresponding to Eq.35.

Table 1 the characteristic of EMULSTAR 3000 UG

SGe (kg/m^3) density of the explosive	VOD(s) velocity of detonation	$P_d(GPa)$ detonation pressure	d_c (mm) diameter of the explosif	d_h (mm) blasthole diameter	$t_r(s)$ to pressure reach peak time
1.25	5600	9.9	80	165	0.0003361

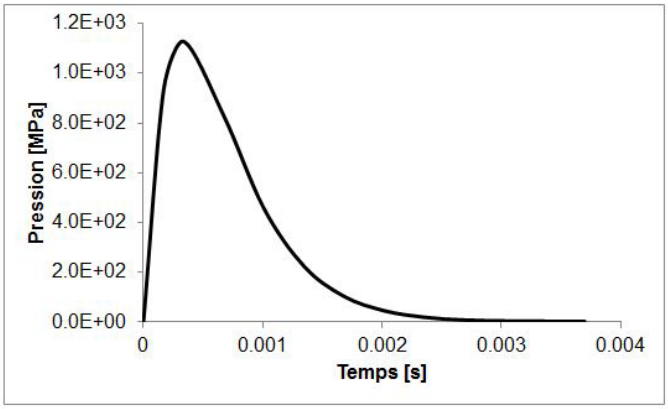

Fig.3. Blast pressure time history used in the simulations.

6.2 Geometrical modeling

We have considered a bench blast model in 2D. To obtain a detonation wave pressure and more precise explosion, the geometric model requires a very fine mesh near the borehole charge. The mesh comprises a total of 4080 elements. A progressive mesh refinement was performed as follows: until 100 mm from the borehole center the mesh counts 1600 elements. From 100 to 500 mm from the borehole center, mesh refinement is reduced to 800 elements. This mesh refinement provides an appropriate transition to better represent the phenomena near the borehole charge (where they are strongest) as in (Li et al. (2009)). Free boundary conditions have been considered for the external boundaries (see Fig.4). Blast pressure is applied in the borehole (see Fig.3). The numerical values of the parameters used in the simulations are given in Table 2. They represent the reference parameters of the numerical simulations performed below. However, in order to study the influence of the key parameters of the model, the following sub-sections consider varying values of ε, d_0 and θ

Table 2 Numerical values of parameters used in the simulations

E(Pa)	υ(-)	$\varepsilon(m)$	$\rho(kg/m^3)$	$d_0(-)$	$\mathcal{G}^c(jm^{-2})$	θ
$2.\ 10^9$	0.3	1.10^{-3}	1400	0.2	164	90°

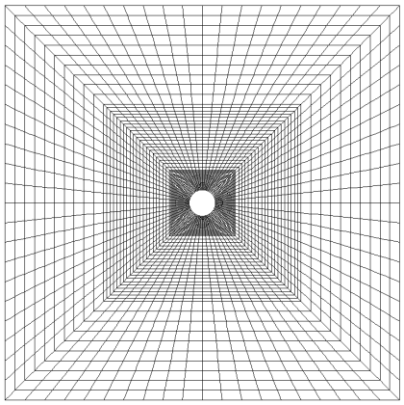

Fig.4. Geometrical model and mesh.

7. Numerical results

Fig. 5 shows damage distribution around the borehole charge for different explosion times. The developed model takes exclusively into account the crack propagation in tensile mode (Mode I). Consequently, radial fractures zone is due to the orthoradial tensile stresses which are perpendicular to the direction of crack propagation. This is why the damage is greater in the vertical direction. The micro-cracks orientation is 90° in this simulation. At t= $2.85*10^{-4}$ seconds non-uniformity of the radial fractures are observed (Fig. 5). This non-uniformity of radial fractures is due to shear stresses in the elements of the mesh. This shear depends on the detonation pressure (see Fig.3) that increases up to t = $3.36*10^{-4}$ seconds and decreases after this time. In the references related to cracks axes (horizontal and vertical axes), the maximum value of shear is find in half of each quarter of the circumference of the borehole charge. In the others words in the diagonal position of the geometry (45°, 135°, 225° et 315°). In these positions, the projections of the resulting shear stress in the elements on these axes have horizontal components which are perpendicular to cracks and which act in tension. This makes cracks to propagate in mode I. This is the reason why the damage is more important in the diagonal direction of the geometry. To highlight the effect of this shear stress, Fig.6 shows the shear stress evolution map with a zoom scale. This map illustrates that the shear is well intense is in the directions mentioned above that is to 45°, 135°, 225° and 315°).

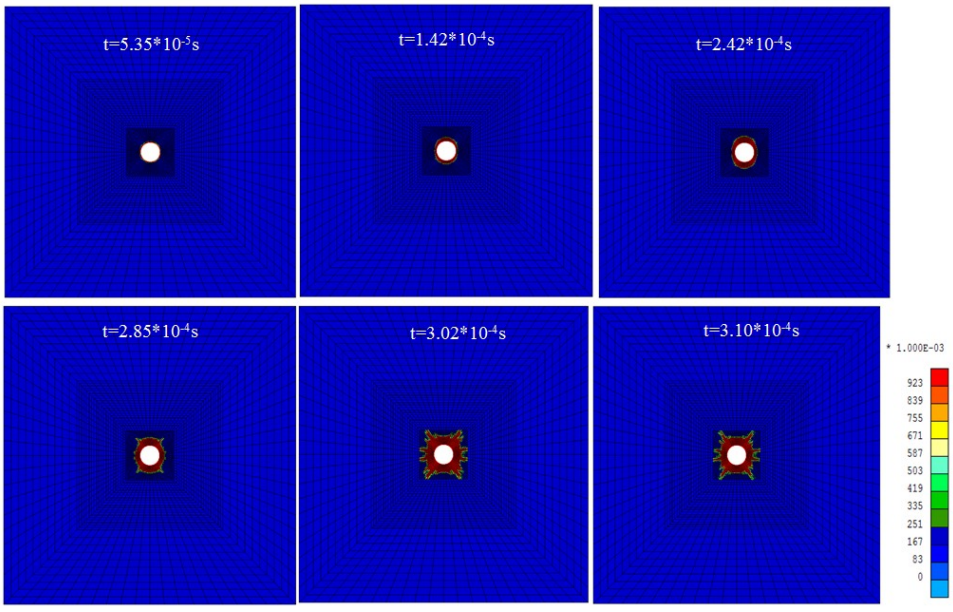

Fig.5. Damage distribution around borehole charge for differents explosion time

The Fig.7 shows the damage distribution around borehole charge for different micro-cracks orientation (0°,90°,30°). We can see that damage distribution for the orientation of 0° is symmetric to that for the orientation of 90°.

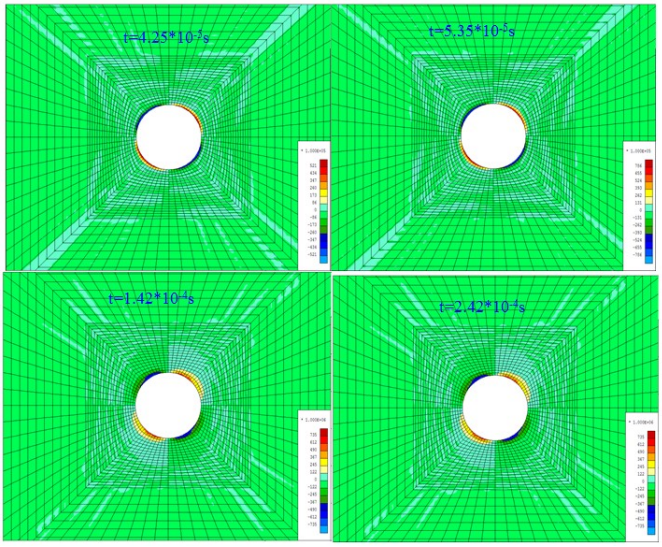

Fig.6. Shear stress evolution map during blasting.

We also study the influence of microstructual size ε on the damage distribution. To do so, we performed some simulations for three different microstructual sizes: $\varepsilon = 5 * 10^{-4}$ m , $\varepsilon = 1 * 10^{-3}$ m and $\varepsilon = 5 * 10^{-3}$ m. We find that the smaller the microstructual size ε is, the more limited is the damage zone at the same moments of explosion (see Fig.8).

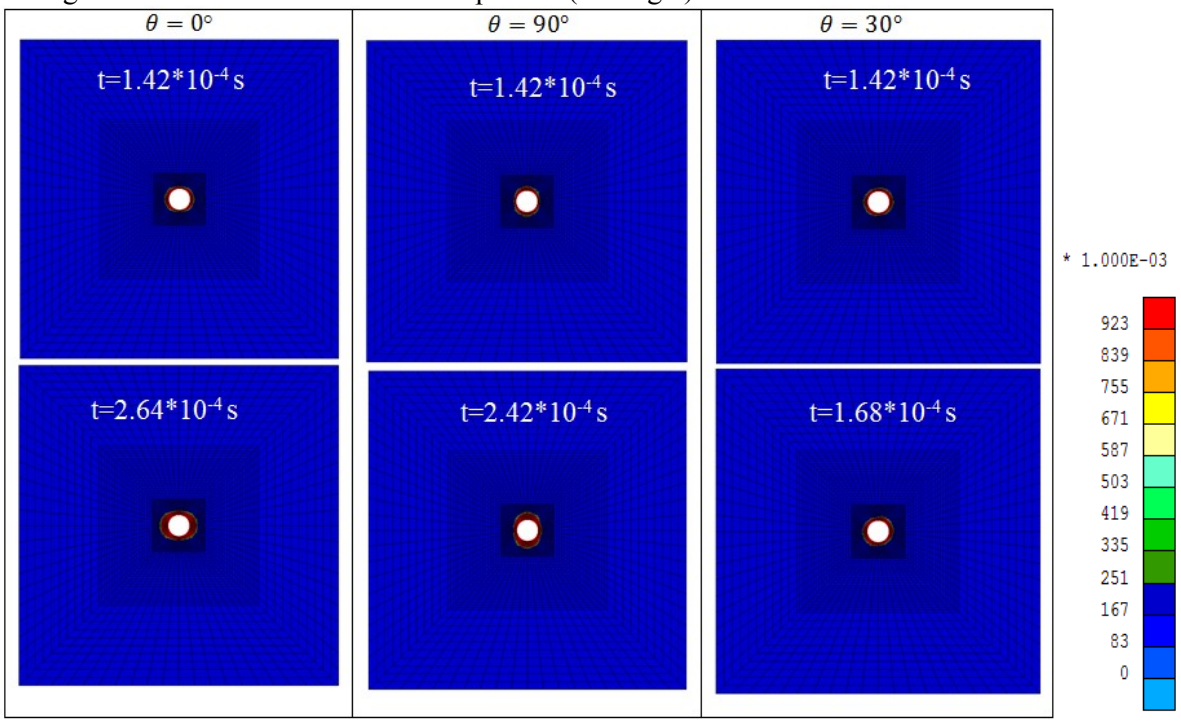

Fig.7. Damage distribution around borehole charge for différents micro-cracks orientation: $\theta = (0°, 90° \ and \ 30°)$

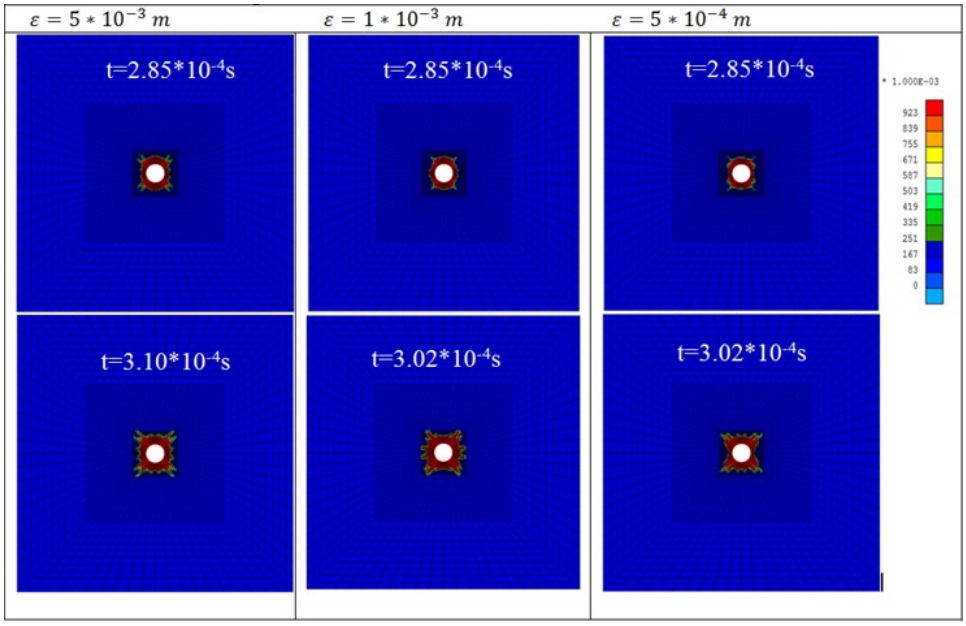

Fig.8. Damage distribution around borehole charge for differents microstructual size $\varepsilon: = 5 * 10^{-4}\, m$, $\varepsilon = 1 * 10^{-3}\, m$ and $\varepsilon = 5 * 10^{-3}\, m$.

8. Conclusions

In this work a two-scale model for blasting damage in tension has been developed. We have shown that the model is capable of reproducing the radial fractures zone due to orthoradial tensile stresses. The influence of the microstructural size and the orientation of the micro-cracks on damage distribution have been studied. It was shown that these parameters have an significant influence on damage distribution.

Acknowledgements

O. Keita acknowledges the Fonds David et Alice Van Buuren for the financial support of this work.

References

Bensoussan, A., Lions, J. and Papanicolaou, G., 1978, Asymptotic Analysis for Periodic Structures. *Kluwer Academic Publisher, Amsterdam.*

Brace, W.F. and Bombolakis, E.G,1963, A note on brittle crack growth in compression. *J. Geophys. Res., 68: 3709–3713.*

Cho, S. H. and Kaneko, K., 2004, Rock Fragmentation Control in Blasting, *Materials Transactions., Vol. 45, No. 5 (2004) pp. 1722-1730.*

Dascalu, C., Bilbie, G. and Agiasofitou, E, 2008, Damage and size effect in elastic solids: *A homogenization approach. Int. J. Solid Struct., 45: 409–430.*

Freund, L.B., 1998, Dynamic Fracture Mechanics, Cambridge University Press.

Keita, O., Dascalu C., Francois B. 2014. A two-scale model for dynamic damage evolution, *Journal of the Mechanics and Physics of Solids., 64: 170–183.*

Langefors, U. and Kihlstrom, B.,1978, The modern technique of rock blasting, *John Wiley & Sons Inc ; 3rd edition.*

Li, C., Kang, L., Qi, Q., Mao, D., Liu, Q. and Xu, G., 2009, The numerical analysis of borehole blasting and application in coal mine roof-weaken, *Procedia Earth and Planetary Science*.

Sanchez-Palencia, E., 1980, Non-homogeneous Media and Vibration Theory, *Lecture Notes in Physics., vol.127, Springer, Berlin.*

Konya, CJ, Walter, EJ, 1991, Rock blasting and overbreak control. *FHWA-HI-92-001, National Highway Institute, 5 pp*